SYNTHESIS, CHARACTERIZATION, CYTOTOXICITY, AND ANTIMICROBIAL ACTIVITY OF AZOBENZENE-IMIDAZOLIUM IONIC LIQUID CRYSTALS

BABAMALE HALIMAH FUNMILAYO

UNIVERSITI SAINS MALAYSIA

2023

SYNTHESIS, CHARACTERIZATION, CYTOTOXICITY, AND ANTIMICROBIAL ACTIVITY OF AZOBENZENE-IMIDAZOLIUM IONIC LIQUID CRYSTALS

by

BABAMALE HALIMAH FUNMILAYO

Thesis submitted in fulfillment of the requirements
for the degree of
Doctor of Philosophy

April 2023

ACKNOWLEDGEMENT

All praise and adoration to Allah, the most beneficent and merciful, for His bounties and mercy in keeping me well enough to begin and complete my PhD programme.

I am grateful to my exceptional supervisor, Dr Yam Wan Sinn, for her resourceful and immeasurable support, opportunities, and trust. I appreciate her allowing me to benefit from her vast knowledge and ideas, as well as her constructive criticism, which has helped me better my research abilities, adaption, and coping methods. She painstakingly read, corrected, reviewed, and edited my thesis, offering useful ideas along the way. Thank you, Dr.

My parents, Alhaji Issaka Shehu and Rofiat Shehu, and parents in-love, Alh Abdulmalik Babamale and Alhaja Waseelah Babamale deserve special recognition and gratitude for inspiring me to achieve this level of accomplishment and pursue my passion. My accomplishment would not have been possible without the financial and emotional assistance, support, and love of my husband, Alh. Kassim Kayode Babamale, and my darling children Royhanah, Hamzat, Fatimah-Zahrah, Waseelah Babamale and Rahmah Murtala. I am grateful to my siblings Hajia Maryam Yusuf, Mrs. Hamidat Adua Uthman, Miss Nihmah Shehu and every member of my family for their prayers and unwavering support throughout this journey.

My heartfelt gratitude and appreciation are directed to Prof.&Dr. Mrs. Oloyede and family, Prof.&Dr. Mrs. Ambali and family, my sis and friends, Amina Owodunni and mother (Hajia Fatimah Owodunni), Mrs Bola Sagaya Yusuf, Mrs Rasheedah Babamale-Adeta, Mrs Waseelah Aiyelabegan and Alh Suleiman Abdulsalam Tapa may Allah reward their families abundantly. Br. Kale Adebayo, Br. Rasheed Dauda,

Br. AbdulRasheed Kainji, Br. Saliu Bioku-Chairman, Br. Saliu Amasa, Sis. Medinat Shade Babata, Lateefah Issa, for their unspeakable encouragement and moral support. I'd like to express my gratitude to Kassim Tanzania, Mohammad Jordan, Bazri and all my study roommates, Dr Olaiya, Mrs Samirah Adebayo, Dr. Fatimah Shittu, Dr Saidat Olaniran, Mrs Maryam Abdurraheem and to my Malaysian family Dr. Syahida Farhan Azha, Nur Farah Hani and all others who became friends and family throughout my time at USM. Thank you for your unflinching support during difficult times and for the wonderful memories we shared. Thank you for your help, support, and guidance during my studies.

I want to express my gratitude to my colleagues turn family, Dr. Ibrahim Ayinla Kuranga, Dr. A.O Rajee, Dr. Mrs. T. O. Abu, Dr. Mrs. A.A Muhammed, Mrs. Fatimah Ajikobi, my wonderful mentors and elders, Prof. N. AbdusSalam, Prof. B.A. Alafara, Prof. Mrs Oluwaniyi, Dr. A. Lawal, Dr. F.O Okeola, Dr. M. O. Ameen, Dr. H.K. Okoro, Dr. H. I. Adegoke and the entire staff of Chemistry and Industrial Chemistry departments in the University of Ilorin. I am grateful to the other Professors, laboratory and administrative staffs, and colleagues in the School of Chemical Sciences who made my academic pursuit at Universiti Sains Malaysia (USM) beneficial, enjoyable, and aided the research project's success.

Finally, many thanks to UNILORIN, TETFUND Nigeria, and Universiti Sains Malaysia (USM) for providing research funding and support through the Research University Grant helping me complete a successful research project. Thank you.

Halimah Funmilayo Babamale,

Chemical Sciences, USM,

March 2023

TABLE OF CONTENTS

ACKNOWLEDGEMENT ..... **ii**

TABLE OF CONTENTS ..... **iv**

LIST OF TABLES ..... **vii**

LIST OF FIGURES ..... **ix**

LIST OF SCHEMES ..... **xiv**

LIST OF SYMBOLS AND ABBREVIATIONS ..... **xv**

ABSTRAK ..... **xvi**

ABSTRACT ..... **xviii**

CHAPTER 1 INTRODUCTION **1**

1.1 Background of Study 1

1.1.1 Bioactive lyotropic and thermotropic LCs and ILCs 3

1.1.2 Fluorinated Liquid Crystals and Bioactivity of Fluorinated Compounds 7

1.2 Problem statement 8

1.3 Research Objectives 10

1.4 Scope of Research Work 10

CHAPTER 2 LITERATURE REVIEW **12**

2.1 An overview of liquid crystals (LCs) and ionic liquid crystals (ILCs) 12

2.1.1 Classification of ILCs: Lyotropic and Thermotropic 14

2.1.2 Classification of mesophase: smectic, columnar, cubic phases 15

2.2 Effects of fluorination on LC properties 16

2.3 Azobenzene based LCs and ILCs 18

2.3.1 Azobenzene-imidazolium ILCs 27

2.4 Imidazolium ILCs 30

2.5 Applications of ILCs 31

2.6 Biological relevance of LCs and ILCs 32

2.7 Biological activities of azobenzene derivatives 35

2.7.1 Anticancer activities of azobenzene derivatives 35

2.7.2 Antimicrobial activities of azobenzene derivatives 38

2.8 Biological activities of imidazolium salts 40

2.8.1 Anticancer activities of imidazolium salts 40

2.8.2 Antimicrobial activities of imidazolium salts 44

2.9 Effect of fluorination on biological activities 47

CHAPTER 3 METHODOLOGY 51

3.1 Chemicals and materials 51

3.2 Characterization 51

3.2.1 Infrared Spectroscopy 51

3.2.2 Nuclear Magnetic Resonance Spectroscopy 52

3.2.3 CHN Elemental Analysis 52

3.2.4 Melting Point Determination 52

3.2.5 Differential Scanning Calorimetry (DSC) 52

3.2.6 Polarized Optical Microscopy (POM) 52

3.3 Biological studies 53

3.3.1 MTT Assay 53

3.3.2 Disc Diffusion Method 54

3.4 Synthesis of azobenzene intermediates 55

3.4.1 Synthesis of *N*-[4-(decyloxy)phenyl]acetamide, 1 55

3.4.2 Synthesis of 4-(decyloxy)aniline, 2 56

3.4.3 Synthesis of (*E*)-4-((4′-(decyloxy)phenyl)diazenyl)phenol/fluorinated phenols, 3-5 57

3.4.4 Synthesis of (*E*)-*N*-(4-bromohexyl)oxy)phenyl)-*N*′decyloxy)phenyl/ difluorinated phenyl)diazenes, 6-7 58

3.5 Synthesis of azobenzene-imidazolium salts 62

3.5.1 Synthesis of (*E*)-*N*-alkyl-*N′*-6-(4-(4′-decyloxyphenyl)diazenyl)phenoxy) hexan-1-imidazolium bromides, 9a-9e 63

3.5.2 Synthesis of (*E*)-*N*-alkyl-*N′*-6-(4-(4′-decyloxyphenyl)diazenyl)-2,6-difluorophenoxy)-hexan-1-imidazolium bromides, 10a-10e 66

3.5.3 Synthesis of (*E*)-*N*-alkyl-*N′*-6-(4-(4′-decyloxyphenyl)diazenyl)-2,3,5,6 tetrafluorophenoxy)hexan-1-imidazolium bromides, 11a-11e 69

3.5.4 Synthesis of (*E*)-*N*-hexadecyl-*N′*-6-(4-(4′-decyloxyphenyl)diazenyl)- 2,3,5,6-tetrafluorophenoxy)-propan-1-imidazolium bromide 12a-12j 73

CHAPTER 4 RESULT AND DISCUSSION 79

4.1 Synthesis 79

4.2 Characterization 81

4.2.1 FTIR Spectral Analysis 81

4.2.2 NMR Spectral Analysis 82

4.3 Phase properties and thermal behavior 115

4.4 Biological Activity Study 128

4.4.1 In Vitro Cytotoxicity Investigation 128

4.4.2 Antimicrobial Activity 134

CHAPTER 5 CONCLUSION AND RECOMMENDATION 140

5.1 Conclusions 140

5.2 Recommendation 143

REFERENCES 145

APPENDICES

LIST OF PUBLICATIONS

LIST OF TABLES

Page

Table 4.1 CHN microanalytical data of compounds **9a-9e, 10a-10e, 11a-11e,** and **12a-12j** 80

Table 4.2 ^{1}H-^{13}C correlations as inferred from the expanded 2D HSQC and HMBC spectral analysis for **9c** 96

Table 4.3 ^{1}H-^{13}C correlations as inferred from the expanded 2D HSQC and HMBC spectral analysis for **10b** 114

Table 4.4 ^{1}H-^{13}C correlations as inferred from the expanded 2D HSQC and HMBC spectral analysis for **11b** 114

Table 4.5 ^{1}H-^{13}C correlations as inferred from the expanded 2D HSQC and HMBC spectral analysis for **12h** 114

Table 4.6 Phase transition temperatures (°C) and associated enthalpy change values (kJ mol^{-1}) of monoalkylated internediates, **3-5** and dialkylated intermediates, **6,7, 8a-8j** determined by DSC at a heating and cooling rate of 5 °C min^{-1} 115

Table 4.7 Phase transition temperatures (°C) and enthalpy change values (kJ mol^{-1}) of **9a-9e,** determined by DSC at a heating and cooling rate of 5 °C min^{-1} 120

Table 4.8 Phase transition temperatures (°C) and enthalpy change values (kJ mol^{-1}) of **10a-10e** determined by DSC at a heating and cooling rate of 5 °C min^{-1} 121

Table 4.9 Phase transition temperatures (°C) and enthalpy change values (k*J* mol^{-1}) of **11a-11e** determined by DSC at a heating and cooling rate of 5 °C min^{-1} 122

Table 4.10 Phase transition temperatures (°C) and enthalpy change values (kJ mol^{-1}) of **12a-12j** determined by DSC at a heating and cooling rate of 5 °C min^{-1} 123

Table 4.11 The half maximal inhibitory concentration (IC_{50}) and selectivity indices of the azobenzene-imidazolium salts, **9a-9e, 10a-10e, 11a-11e and 12a-12j**, and Etoposide on HeLa cells and Hs27 fibroblasts at 24 h as determined using the MTT assay. 130

Table 4.12 Zone of Inhibition obtained for tested compounds using Kirby-Bauer disc diffusion method. 136

LIST OF FIGURES

Page

Figure 2.1 Cholesteryl acetate (**1**) and Cholesteryl benzoate (**2**) the first reported liquid crystals (Furrer, 2021; Pérez-Hernández et al., 2018). 13

Figure 2.2 *N*-(n-alkyl)-pyridinium halides, the first reported ILCs (Knight & Shaw, 1938). 13

Figure 2.3 Chemical structure of some aromatic cationic head groups..... 14

Figure 2.4 Lateral fluorinated alkoxyl benzoic acid (Gray, 1964). 17

Figure 2.5 Fluorine-substituted benzoate esters linked to an azobenzene core with a terminal double bond (Rahman et al., 2014). 18

Figure 2.6 Lateral fluoro-substituted terphenyls (Haouas et al., 2021). 18

Figure 2.7 Chemical structure of azobenzene (Merino, 2011) 19

Figure 2.8 Chemical structure of ammonium-containing azobenzene ILCs with enhanced phase stability (Ujiie & Iimura, 1992) 21

Figure 2.9 Neutral and azobenzene ILCs containing cationic ammonium head group and a chiral hydrogentartrate as the anion (Ujiie & Iimura, 1994) 22

Figure 2.10 Neutral and cationic N-2-hydroxyethylpiperidinium containing azobenzene ILCs (Ujiie et al., 2006)..... 23

Figure 2.11 T-shaped azobenzene ILCs prepared by Li and co-workers (Li et al., 2009). 24

Figure 2.12 Chemical structures of azobenzene-guanidinium ILCs (Wuckert et al., 2015)..... 24

Figure 2.13 Azobenzene-imidazolium ILCs (Kapernaum et al., 2016) 25

Figure 2.14 Azobenzene-guanidinium, azobenzene-amidinium ILCs prepared by Kapernaum et al (2018)..... 26

Figure 2.15 Azobenzene-ammonium ionic derivatives with varying substituents on the cationic head (Sunil et al., 2019). 27

Figure 2.16 Monocationic and dicationic Azobenzene-imidazolium salts (Zhang, et al., 2008a; Zhang, et al., 2008) 28

Figure 2.17 Vinylimidazolium based azobenzene ILCs with enhanced smectic phase stability (Zhang et al., 2011) 29

Figure 2.18 Mono and dicationic azobenzene-imidazolium salts (Stappert et al., 2015)..... 30

Figure 2.19 First reported imidazolium based ILCs (Bowlas et al., 1996). 31

Figure 2.20 Imidazolium based ILCs that could transfect SiRNA (Dobbs et al., 2009). 34

Figure 2.21 Ethoxyether functionalized imidazolium based ILCs with antibacterial activities Huang and co-workers (Huang et al., 2011) .. 34

Figure 2.22 Guanidinium based ILCs containing Tyr (**62)** and Phe (**63**) moieties with antibacterial and cytotoxic activities (Neidhardt et al., 2018)..... 35

Figure 2.23 Azobenzene prodrugs (Sharma et al., 2013) 36

Figure 2.24 Schiff base-containing cytotoxic aryl azo and azoxy derivative (Su et al., 2015)..... 37

Figure 2.25 Azobenzene derivative with anti-pancreatic cancer activities (Shinzawa et al., 2021)..... 37

Figure 2.26 Trypan red™ (**69**) and Prontosil™ (**70**), the first discovered aryl azo derived anti-parasitic and antibacterial drugs, respectively (Ehrlich, 1913; Valent et al., 2016)..... 38

Figure 2.27 Azobenzene derivatives with antimicrobial activities (Concilio et al., 2017; Piotto et al., 2017). 39

Figure 2.28 Bioactive amphiphilic azobenzene-ammonium salts (Franche et al., 2020). 40

Figure 2.29 Chemical structures of compounds with selective anticancer effects (Zhang et al., 2017). 41

Figure 2.30 Structures of selected C^2-alkyl substituted derivatives of imidazolium salts (DeBord et al., 2017). 42

Figure 2.31 Chemical structures of some acridine-based imidazolium salt derivatives with selective cytotoxicity (Sharhan et al., 2018). 43

Figure 2.32 Chemical structure of bis-imidazolium salts with high cytotoxicity (Southerland et al., 2021) 44

Figure 2.33 Steroid-based imidazolium salts with selective antibacterial and antifungal activities (Hryniewicka et al., 2019). 45

Figure 2.34 Benzoates series with antimicrobial potentials (Satheesh et al., 2020). 46

Figure 2.35 Imidazolium salts with different anionic components exhibiting different cytotoxicity (Zulikha et al., 2014). 47

Figure 2.36 Imidazolium salts with different anions (Debord et al., 2017). 47

Figure 2.37 Chemical structures of fluorinated benzothiazolyl trimethine cyanines (Ge et al., 2012).....49

Figure 2.38 Fluorinated substituted sulfonylaminobenzamide derivative (Li et al., 2014). 50

Figure 2.39 Chemical structure of a cytotoxic fluorinated benzimidazole derivative (Reddy et al., 2015). 50

Figure 4.1 FTIR spectra of compounds (a) **3**, (b) **6** and (c) **9c**. 82

Figure 4.2 ^{1}H NMR spectrum of compound **3** 84

Figure 4.3 Structure of compound **9c**, with complete atomic numbering. 85

Figure 4.4 Structure of compound **10b**, with complete atomic numbering.....85

Figure 4.5 Structure of compound **11b**, with complete atomic numbering.....86

Figure 4.6 Structure of compound **12h**, with complete atomic numbering.....86

Figure 4.7 ^{1}H NMR spectrum of compound **9c**.....88

Figure 4.8 ^{1}H-^{1}H COSY spectrum of compound **9c**.....90

Figure 4.9 ^{13}C NMR spectrum of compound **9c**.....92

Figure 4.10 Expanded ^{1}H-^{13}C HSQC spectrum (3.3-11.5 ppm) of compound **9c** 94

Figure 4.11 Expanded ^{1}H-^{13}C HMBC spectrum (3.5-11.5ppm) of compound **9c** 95

Figure 4.12 ^{1}H NMR spectrum of compound **10b** 97

Figure 4.13 ^{1}H NMR spectrum of compound **11b** 98

Figure 4.14 ^{1}H NMR spectrum of compound **12h** 99

Figure 4.15 ^{1}H-^{1}H COSY spectrum of compound **10b** 101

Figure 4.16 ^{1}H-^{1}H COSY spectrum of compound **11b** 102

Figure 4.17 ^{1}H-^{1}H COSY spectrum of compound **12h** 103

Figure 4.18 ^{13}C NMR spectrum of compound **10b** 105

Figure 4.19 ^{13}C NMR spectrum of compound **11b** 106

Figure 4.20 ^{13}C NMR spectrum of compound **12h** 106

Figure 4.21 Expanded ^{1}H-^{13}C HSQC spectrum (3.5-11.5 ppm) of compound **10b** 108

Figure 4.22 Expanded ^{1}H-^{13}C HMBC spectrum (3.5-11.5 ppm) of compound **10b** 109

Figure 4.23 Expanded ^{1}H-^{13}C HSQC spectrum (3.5-11.5 ppm) of compound **11b** 110

Figure 4.24 Expanded ^{1}H-^{13}C HMBC spectrum (3.5-11.5 ppm) of compound **11b** 111

Figure 4.25 Expanded ^{1}H-^{13}C HSQC spectrum (3.5-11.5 ppm) of compound **12h** 112

Figure 4.26 Expanded ^{1}H-^{13}C HMBC spectrum (3.5-11.5 ppm) of compound **12h** 113

Figure 4.27 DSC traces of compounds **3** (top), and **6** (bottom) 117

Figure 4.28 (a) Focal conic fan texture of SmA phase seen in compound **6** at 83.5 ℃; (b) Focal fan texture of SmA phase observed for compound **7** at 44.3 ℃ upon cooling. 118

Figure 4.29 A DSC trace of compound **9c** 120

Figure 4.30 A DSC trace of **10b** (left), and **11c** (right).....122

Figure 4.31 DSC trace of compound **12h**.....124

Figure 4.32 Co-existence of dark domains and filament texture observed in compound **9c** at 149.8 ℃ during heating. 125

Figure 4.33: Co-existence of dark domains and broken focal conic fan texture of SmA phase observed in **10b** at 87.3 ℃ upon cooling. 126

Figure 4.34 (a) Schlieren texture of SmC phase observed in **12a** at 100.8 ℃ upon cooling (b) Broken fan texture of SmA observed for **12h** at 97.5 ℃ upon cooling.....127

Figure 4.35 (a) Inhibition zone of vancomycin, ampicillin and streptomycin against the respective organisms. (b) Inhibition zone of compounds **9c** (left)**, 10b** (middle) and **12h** (right) against *S. aureus* (c) Inhibition zone of compounds **9c** (left)**, 10b** (middle) and **12h** (right) against *E. coli* and (d) Inhibition zone of compounds **9c** (left)**, 10b** (middle) and **12h** (right) against *C. albicans*. 138

LIST OF SCHEMES

Page

Scheme 3.1 Synthesis routes toward the formation of fluorinated/non-fluorinated azobenzene intermediates. Reagents and conditions: (i) K_2CO_3/acetone, 1-bromodecane, reflux 24 h; (ii) NaOH/ethanol, reflux 24 h; (iii) cooled HCl conc. (aq); cooled $NaNO_2$ (aq), stirred for 1 h; cooled phenol/2,6-difluorophenol/2,3,5,6-tetrafluorophenol, stirred at 0-5 °C for 2 h. (iv) K_2CO_3/acetone, dibromoalkanes, reflux 6 h (Sunil et al., 2019). 55

Scheme 3.2 Synthesis routes toward the formation of fluorinated/non-fluorinated azobenzene-imidazolium salts. Reagents and conditions: (i) *N*-alkyl imidazole/acetone, reflux for 48 h. (Sunil et al., 2019). 62

LIST OF SYMBOLS AND ABBREVIATIONS

DCM	Dichloromethane
$CDCl_3$	Deuterated chloroform
MTT	(3-[4,5-dimethylthiazol-2-yl]-2,5 diphenyl tetrazolium bromide)
MHB	Muller-Hinton agar
FTIR	Fourier Transform infra-red spectroscopy
NMR	Nuclear magnetic resonance spectroscopy
^{1}H NMR	Proton nuclear magnetic resonance spectroscopy
^{13}C NMR	Carbon nuclear magnetic resonance spectroscopy
COSY	Correlated spectroscopy
HSQC	Heteronuclear single quantum coherence
HMBC	Heteronuclear multiple bond correlation
%	percentage
°C	degree Celcius
mp	melting point
1D	one dimensional
2D	two dimensional
d	doublet
Hz	hertz
J	coupling constant
µM	micro mole
µg	microgram
h	hour(s)
m	multiplets
ppm	parts per million
s	singlet
t	triplets

SINTESIS, PENCIRIAN, SITOTOKSISITI DAN AKTIVITI ANTIMIKROB BAGI HABLUR CECAIR IONIK AZOBENZENA-IMIDAZOLIUM

ABSTRAK

Empat siri garam azobenzena-imidazolium baharu telah disintesis melalui gandingan azo diikuti oleh pengalkilan dan kuaternisasi azobenzena dengan imidazole-*N*-teralkil yang mempunyai pelbagai rantai panjang untuk menghasilkan garam yang tidak terfluorinan (**9a-9e**), difluorinan (**10a-10e**) dan tetrafluorinan (**11a-11e, 12a-12j**). Ketulenan sebatian telah disahkan oleh analisis unsur CHN dan struktur kimia sebatian ini ditentukan dengan menggunakan spektroskopi inframerah (FTIR), 1D dan 2D resonan magnet nuklear (NMR). Sifat hablur cecair sebatian tersebut telah dikaji dengan menggunakan kalorimetri imbasan pembezaan (DSC) dan mikroskop optik terkutub (POM). Sitotoksisiti secara *in vitro* telah dinilai menggunakan ujian MTT dan aktiviti antimikrob telah disiasat menggunakan kaedah penyebaran cakera. Fasa smektik A (SmA) diperhatikan dalam hampir semua sebatian. Bagi sebatian tidak terfluorinan, panjang rantai alkil terminal minimum yang diperlukan untuk mendorong sifat hablur cecair ialah empat belas karbon, dan sepuluh atom karbon diperlukan dalam analog terfluorinan. Suhu pembersihan (Tc) meningkat dengan peningkatan dalam panjang rantaian alkil yang membawa kepada julat mesofasa yang lebih luas dapat diperhatikan untuk sebatian **9e, 10e**, dan **11e** (n = 18). Dengan mempelbagaikan pengatur jarak alkoksi **11d** daripada tiga hingga dua belas pengatur karboamn untuk mendapatkan **12a-12j**, fasa smektik C (SmC) diperhatikan untuk **12a-12c** (m = 3-5). Tc untuk sebatian **12a-12h** (m = 3-10) menurun dengan peningkatan spaser alkil. Secara amnya, fluorinasi menurunkan suhu lebur (Tm) dalam kesemua analog.

Sitotoksisiti sebatian terhadap sel HeLa dipengaruhi oleh rantai panjang alkil terminal pada imidazolium, panjang spaser dan fluorinasi, yang mana dengan analog terfluorinan adalah lebih aktif berbanding dengan analog tidak terfluorinan, dan homolog terpanjang dalam setiap siri: **9e** (IC_{50} = 1.17 µM), **10e** (IC_{50} = 1.26 µM) dan **11e** (IC_{50} = 0.61 µM), (n = 18) menunjukkan peningkatan dalam aktiviti sitotoksik. Apabila panjang spaser **11d** dipelbagaikan, sitotoksisiti dalam sebatian **12a-12j** meningket (m = 3-12, IC_{50} = 1.74-12.42 µM). Kesemua garam adalah lebih mujarab berbandingkan dengan etoposide (IC_{50} = 25.67 µM). Selektiviti sebatian terhadap Hs27 didapati meningkat dengan peningkatan panjang rantai alkil terminal atau spaser. Sebatian **12f** (m = 8, S.I = 11.03) ialah sebatian yang paling selektif. Aktiviti antimikrob bagi garam berkait rapat dengan morfologi sel organisma yang diuji iaitu (*Staphylococcus aureus* (*S.aureus*), *Escherichia coli (E. coli), Salmonella enterica serovar Typhimurium* (*Salmonella*), *Candida albicans (C. albicans)* dan *Saccharomyces cerevisiae* (*Saccharomyces*), dan peningkatan hidrofobisiti/lipofilisiti dalam rantaian alkil yang meningkatkan kebolehtelapan ke dalam membran sel mikrob. Sebatian didapati selektif dalam aktivitinya terhadap setiap organisma. Penambahan atom fluorin meningkatkan ketersediaan bio siri berfluorinasi.

SYNTHESIS, CHARACTERIZATION, CYTOTOXICITY AND ANTIMICROBIAL ACTIVITY OF AZOBENZENE-IMIDAZOLIUM IONIC LIQUID CRYSTALS

ABSTRACT

Four new series of azobenzene-imidazolium salts were synthesized by azo coupling, followed by alkylation and subsequent quaternization of *N*-alkylated imidazoles of various chain length with azobenzenes to afford the non-fluorinated (**9a-9e**), difluorinated (**10a-10e**) and tetrafluorinated (**11a-11e, 12a-12j**) salts. The purity of the compounds was confirmed by CHN elemental analysis and their structures were elucidated using the FTIR, 1D and 2D NMR spectroscopies. The liquid crystalline (LC) properties of the salts were studied using the DSC and POM. *In vitro* cytotoxicity was explored using the MTT assay and their antimicrobial activities were investigated using the disc diffusion method. Smectic A (SmA) phase was observed in almost all compounds. In non-fluorinated analogues, the minimum terminal alkyl chain length required to induce LC properties was fourteen carbons, and ten carbon atoms in the fluorinated analogues. The clearing temperature (T_c) increased with an increase in alkyl chain length leading to a wider mesophase range observed for compounds **9e**, **10e**, and **11e** (n = 18). By varying the alkoxyl spacer of **11d** from three to twelve carbon spacers to obtain **12a-12j**, the smectic C (SmC) phase was observed for **12a-12c** (m = 3-5). T_c for compounds **12a-12h** (m = 3-10) decreased with an increase in alkoxyl spacer. Generally, fluorination decreased the T_m in all analogues. The cytotoxicity of the salts against HeLa cells was influenced by the length of the terminal alkyl chain on the imidazolium head, spacer length and fluorination. The fluorinated analogues being more active than non-fluorinated, and longest homologs in each series

9e (IC_{50} = 1.17 µM), **10e** (IC_{50} = 1.26 µM), and **11e** (IC_{50} = 0.61 µM), (n = 18) showed most activity. By varying the spacer length of **11d**, increasing the alkyl spacer length increased cytotoxicity in **12a-12j (**m = 3-12, IC_{50} = 1.74-12.42 µM). All salts were more potent than etoposide (IC_{50} = 25.67 µM)**.** The selectivity of compounds against Hs27 was found to increase with increasing terminal alkyl chain length or spacer length. Compound **12f** (m = 8, S.I = 11.03) was found to be the most selective compound. The antimicrobial activity of the salts was strongly related to the cell morphology of the five tested microorganisms (*Staphylococcus aureus* (*S.aureus*), *Escherichia coli (E. coli), Salmonella enterica serovar Typhimurium* (*Salmonella*), *Candida albicans (C. albicans)* and *Saccharomyces cerevisiae* (*Saccharomyces*)), and increased alkyl chain hydrophobicity/lipophilicity, which increased permeability into the microbial cell membrane. The compounds were found to be selective in their activity towards each microorganism. The addition of fluorine atoms increased the bioavailability of the fluorinated compounds.

CHAPTER 1
INTRODUCTION

1.1 Background of Study

Liquid crystals (LCs) are an intermediate state of matter between a crystalline solid and liquid phase (Suthar & Doshi, 2013; Wang et al., 2020). They are mesomorphic forms of matter with dual properties of conventional liquids and solid crystals. LCs are usually anisotropic, and the molecules show long-range and short-range orientational and positional orders. The constituents of LC molecules are usually mesogenic or semi-rigid cores (e.g., phenyl rings) with strong dipoles/easily polarizable substituents and long, flexible terminal alkyl chain(s). They may have rod-like (calamitic), disc-like (discotic), or bent-core (banana shape) molecular structures (Komitov, 2015). Interactions such as dipole-dipole, dipole–induced dipole interactions, hydrogen bonds, or Van der Waals forces existing between mesogenic cores and side chains often induce self-organization in liquid crystalline molecules and thus the formation of LC phases.

LCs can be classified as thermotropic or lyotropic. Lyotropic LCs exhibits mesophase in response to solvent concentration. Lamellar, cubic hexagonal, and tetragonal mesophase are the most common types of mesophases that are exhibited by conventional lyotropic LC. Although these LCs share some basic characteristics with thermotropic LCs, they differ significantly in structure, behaviour, and applications. Lyotropic LC organization is usually based on the interaction between two, or even more, molecular units in solution. As a result, their phase order is determined by the concentrations of the various components added to the mixture. They have been used in dispersal systems due to their ability to self-organize and solubilize as a result of the hydrophilic and hydrophobic /lipophilic properties (Amar-yuli et al., 2009). On the

other hand, mesophase formation in thermotropic liquid crystals are induced by temperature through heating a crystalline solid or cooling a molten mesogen. Their structures usually consist of a rigid and polar central core linked to flexible terminal alkyl chains (Stevenson et al., 2005).

Ionic liquids (ILs) are salts that exists in a liquid state. They usually melt below 100ºC and consist of modifiable cationic and anionic moieties. Chemical modifications influence the distinctive physicochemical properties of ILs, such as viscosity, polarity, thermal and electrochemical stability, melting points and ionic conductivity (Stappert et al., 2015). Changing the combination of cations and anions is a simple way to modify the properties of ILs (Yang et al., 2014). Microphase separation between hydrophobic tails and the hydrophilic heads in ILs often results in a wide range of self-assemble structures (Lombardo et al., 2015; Perkin et al., 2011). The unique properties of ILs makes them suitable for electrolytes in solar cells (electrochemical application), alternative solvents and recently probed as active pharmaceutical agents (Stappert et al., 2015).

Derivatization of LCs (introduction of ionic moiety) or ILs i.e (introduction of long carbon chain to their structure) leads to the development of a new class of amphiphiles known as ionic liquid crystals (ILCs). ILCs comprise of non-covalently bonded cations and anionic components (Mohammad et al., 2021; Yang et al., 2014). They exhibit a rich electrostatic interaction making them uniquely different from neutral LCs. ILCs are an intriguing class of multifunctional hybrid LC and IL materials (Dai et al., 2020; Yang et al., 2014). Similar to LCs, they form an intermediate state of matter between a most ordered crystalline solid and a totally disordered liquid. Their molecules are usually arranged along spatial coordinate(s) (Yang et al., 2014). These

modified LCs exhibit properties such as non-volatility, high thermal stability, high ionic conductivity, and non-flammability, in addition to their ability to self-organize (Binnemans, 2005). These properties contribute to their applications in fields such as material science, optoelectric materials, reaction media and catalysis (Bhattacharjee et al., 2018; Boydston et al., 2007; Gin et al., 2006; Liu et al., 2015) as well as in biological applications (Dobbs et al., 2009; Huang et al., 2011; Neidhardt et al., 2018). Hence, most ILCs have functions similar to those of ILs and LCs and are classified as thermotropic or lyotropic ILCs.

1.1.1 Bioactive lyotropic and thermotropic LCs and ILCs

Cancer is defined as the uncontrolled growth and proliferation of abnormal cells and is a leading cause of death in both developed and developing countries (Cancer, 2020). According to the World Health Organization, it is the second leading cause of mortality worldwide, accounting for one out of every six fatalities. Cervical cancer is one of the most dangerous malignant cancers (Small et al., 2017). This type of cancer is the fourth most common cancer disease in women globally, with an estimated 570,000 new cases and 7.5% of all cancer-related deaths in females in 2018. More than 85% of the estimated 311,000 cervical cancer-related deaths yearly occured in low- and middle-income countries (Ferlay et al., 2018; Stelzle et al., 2021; W.H.O, 2020).

A microbial infection arises when a foreign organism enters the body and multiplies in a harmful manner. Infections can be caused by microorganisms, such as bacteria, viruses, fungus, or parasites. Antibiotics and antifungals drugs have been developed to treat these infections.

Many treatments are available for cancers, such as surgical removal of the tumor or therapies such as chemotherapy, immunotherapy, radiotherapy, hormone therapy, targeted therapies, and stem cell transplant. Currently, radiation, chemotherapy, and surgery are the most prevalent cancer treatments. Chemotherapy is a type of treatment in which chemical agents are used to kill all dividing cells. This is, therefore, a non-targeted treatment. Hence, the clinical efficacy of this treatment has been severely hampered. Similarly, the occurrence of multi-drug resistant microbial strains which emanates from pathogenic bacteria and fungi is one of the major public health threats. Hence, the development of new and efficient antimicrobial agents is imperative (Browne et al., 2020). The unique properties offered by LCs promise for safer, more effective drugs for the treatment of cancer and many other diseases.

Lyotropic liquid crystals have been explored in chemical and biological sensing, solubility enhancement of drugs, dermal application, ophthalmic delivery, colloidal dispersal systems**,** as well as cancer therapeutics, due to their amphiphilic structural features. Their properties are based on microphase segregation of the hydrophilic and hydrophobic components. This class of LCs have many pharmaceutical applications, for example in self-emulsifying systems which increases stability and prolongs hydration, thereby controlled drug delivery due to microphase segregation of incompatible parts (Noguez et al., 2017; Stevenson et al., 2005). Fenoprofen calcium™, ketoprofen™, diclofenac™, salvarsan™, disodium chromoglycate, nafoxidin HCl™, and flufenaminic acid™ are examples of active pharmaceutical ingredients that are lytropic LCs, exhibiting various mesophases, such as nematic, lamellar, cubic, and/or hexagonal (Stevenson et al., 2005). Lyotropic LCs have become interesting formulations for enhancing the delivery system of anticancer agents due to their sensitivity to concentration. They are explored as pH stimuli for

delivery of chemotherapeutics into the acidic environment of tumor cells. For instance, the modification of a basic amphiphile, pyridinylmethyl linoleate produced a pH-responsive lyotropic LC with anticancer properties. The drug delivery efficiency and cytotoxic potential of this lytropic LC was 10- and 3-fold, respectively when compared to that of doxorubicin, an anticancer drug (Negrini et al., 2012). Similarly, the incorporation of docetaxel™ an anticancer drug into phytantriol-functionalised lyotropic LC nanoparticles (NPs) improved the drug delivery efficiency and cytotoxicity against breast cancer cells (MCF-7). Interestingly, these lyotropic LC NPs were less toxic to normal cells relative to that of docetaxel™ (Jain et al., 2015).

Drugs which are thermotropic LCs were also reported. These include anti-inflammatory drugs (fenoprofen™ and leukotriene), antifungal (itraconazole™), antibiotic (tobramycin) as well as anticancer (methotrexate) agents (Bunjes & Rades, 2005; Stevenson et al., 2005). Some conventional thermotropic LCs, for example detirelix™ and nafarelin™ are lead compounds in anticancer therapeutics design due to their high potency against tumor cells and wide safety window. Some of the thermotropic LC anticancer agents, such as methotrexate have been approved for clinical use. (Bunjes & Rades, 2005; Stevenson et al., 2005). Self-assembly of ILCs into lamellar or micellar-like aggregates suggests that they may interact with biological membranes. Molecules within the flexible layers in the smectic C phase are uniformly tilted and exhibits microsegregation of incompatible units (hydrophobic tails) and aggregation of compatible units (hydrophilic heads) or vice versa. This shows strong resemblance with arrangement in the cell membrane containing both hydrophilic and hydrophobic parts. Therefore, the amphiphilic character of this phase, could interact and alter protein and enzyme functions, signaling pathways, lipid distribution, and cell membrane viscoelasticity; generate reactive oxygen species; permeate and disrupt

mitochondria and nuclear membranes, and bind with RNA and DNA of biological materials.

Azobenzene is a common mesogenic core, due to its rigid rod-like shape. The -N=N- group which connects the aromatic rings could enhance the polarizability of the anisotropic azobenzene molecules. They could be modified into thermotropic or lyotropic LCs (Selvarasu & Kannan, 2017; Zhang et al., 2021; Giles et al., 2020; Hara, 2019; Ichimura et al., 2002). Cis-trans isomerization in compounds containing the azo chromophore can be easily induced by irradiation with linearly polarised light. This unique photo switch behavior of azobenzene derivatives have found applications in diverse fields. (Benkhaya et al., 2020; Sunil et al., 2019). Azobenzene derivatives have been used in display electronics and as photo-controllers in biological systems (Dong et al., 2015; Sadovski et al., 2009; Salta et al., 2017; Samanta et al., 2013; Warner et al., 2019). Azo photoswitches have also been applied in drug delivery systems (Abbaszad Rafi et al., 2018). Azobenzene derivatives were reported to exhibit various biological activities such as antineoplastic, antitumor, antiseptic, antimicrobials, antidiabetic and antiandrogenic activities (Concilio et al., 2015; Piotto et al., 2013; Piste et al., 2012; Samper et al., 2017; Sessa et al., 2016; Yazdanbakhsh et al., 2012).

Inspired by the interesting photoresponsive properties and high tunability of neutral azobenzene compounds, azobenzene ionic liquid crystals have been fabricated (Kang et al., 2019; Nam et al., 2020; Stappert et al., 2015; Wuckert et al., 2015). Ionic interactions in ILCs induce micro segregation of hydrophilic and hydrophobic domains and enhanced mesophase stability (Zhang et al., 2008b). Ionic character also significantly influences the mesomorphic behavior, especially the phase transition temperatures. This was observed in azobenzene-ammonium ILCs, wherein

introduction of the ionic moiety was found to lower the melting temperatures and increased the clearing temperatures in these mesogens, thus stabilising a mesophase (as indicated by a broad thermal range) (Ujiie & Iimura, 1992). Amphiphilic azobenzene incorporating different cationic head groups (guanidinium, ammonium, amidinium and imidazolium) with LC properties were also reported (Kapernaum et al., 2018).

Among the many ionic liquid crystalline materials, those based on imidazolium salts are some of the most interesting and frequently investigated amphiphiles (Kapernaum et al., 2016; Stappert et al., 2015; Zhang et al., 2008a). Ionic interactions between the imidazolium moieties tend to stabilize lamellar mesophases. (Yang et al., 2014; Zhang et al., 2008b). The ionic character of the imidazolium moiety has a prominent impact on biological potency. Many imidazolium salts have been found to aid in the reinforcement of affinity and membrane permeability, and consequently have potent anticancer properties (Riduan & Zhang, 2013). Cationic imidazolium salts are useful for increasing affinity, water solubility, and membrane permeability, as well as preventing migration, which improves antimicrobial activity (Coleman et al., 2012; Noujeim et al., 2010). However, this potency could be enhanced by substitution with electron donating or electron withdrawing groups such as the fluorine atom which increases, drug selectivity and lipophilicity, thus resulting in increased antimicrobial activities (Mahmood et al., 2018).

1.1.2 Fluorinated Liquid Crystals and Bioactivity of Fluorinated Compounds

The fluorine atom is small in size, with high electronegativity, and low polarizability. Fluorination could tune the physicochemical properties of liquid crystals. It has a remarkable influence on phase transition temperatures, melting points, as well as mesophase morphology and stability in liquid crystals. Introduction

of fluoro substituents into the mesogenic core, spacer or terminal chains is a feasible route for the synthesis of ILCs (Hird, 2007; Spengler et al., 2017).

On the other hand, fluorination is a common method used in the rationale design of effective therapeutic agents. Research and development of fluorine-containing biological compounds have progressed significantly. Incorporation of this atom could modulate the chemical and biological properties, pharmacodynamics, and pharmacokinetics of organo-compounds (Kosikowska et al., 2021), and thus fluorocarbons have found applications in molecular diagnosis and oncology.

The carbon-fluorine (C-F) bond can be used as a molecular tag in peptide labeling, which is highly important in cancer chemo- and biotherapy. Fluorinated amino acids increase the stability of oligomeric structures in peptide therapeutics, a promising field for emerging anticancer agents (Boohaker et al., 2012; Menaa et al., 2011). Approximately 80% of hitherto reported pharmaceuticals contain fluorine aryl, aromatic trifluoromethyl, or simple fluoroalkyl moiety (Purser et al., 2008). The presence of fluorine atom(s) could increase drugs′ selectivity and lipophilicity, thus resulting in increased antimicrobial activities (Mahmood et al., 2018). Many antitumor agents used in cancer therapy are fluorinated compounds (Cozzi et al., 2004).

1.2 Problem statement

Though chemotherapy is known as one of the most common and effective methods to treat cancer, patients often suffer from adverse side effects of non-targeted chemotherapeutics. Similarly, majority of the existing antibiotics are effective against Gram-positive bacteria but ineffective against the Gram-negative bacteria. In addition, yeasts from the Candida genus also pose serious health risks to humans due to their opportunistic nature. Adherence of these fungi to the surface of human tissues could

cause infections. Therefore, scientists must explore and develop new and selective bioactive agents to overcome this problem.

Lyotropic LCs were reported to have suppressive effects on cancer and bacterial cells due to their molecular arrangement and electronic properties. However, these compounds are dependent on the concentration of system. Hence, their functions and properties may be greatly influenced and compromised in aqueous media. This setback could be overcome by synthesizing solvent-free bioactive thermotropic LCs e.g, fenoprofen. The biological relevance of ILCs, however, is little known. Both azobenzene and imidazolium salts were documented to exhibit anticancer and antimicrobial activities. However, a literature search revealed only limited reports on the anticancer potential of azobenzene derivatives. Fluorination can be used to induce or tune the phase transitional temperature and mesophase morphology in LCs as well as increase lipophilicity and thus the biological potency of organic compounds.

Cytotoxicity effect of organic compounds often correlates directly with their lipophilic properties. Hence in this study, both azobenzene and imidazolium cationic head were functionalized with long alkyl chains. However, azobenzene derivatives with long alkyl chains usually have poor solubility in polar solvents like dimethylsufoxide (DMSO) and water. Incorporation of the ionic imidazolium moiety could improve the solubility of and impart amphiphilic character to the azobenzene component, the latter is essential to facilitate and enhance interaction with bio-membranes. It is expected that ionic interaction of the imidazolium moiety could stabilize the mesophase range and the amphiphilic character it imparts to the azobenzene core could enhance the bio potency of the salts.

1.3 Research Objectives

The objectives of this research are:

i. To synthesize four new series of non-fluorinated and fluorinated amphiphilic azobenzene-imidazolium salts with varying alkyl side chain and spacer lengths.

ii. To characterize the amphiphilic salts using Fourier Transform Infrared (FTIR) spectroscopy and nuclear magnetic resonance (NMR) spectroscopy.

iii. To investigate the phase properties of the amphiphilic salts using differential scanning calorimetry (DSC) and polarized optical microscopy (POM).

iv. To investigate the cytotoxic and antimicrobial potentials of the amphiphilic salts.

1.4 Scope of Research Work

This study explores the synthesis and spectroscopic characterization of azobenzene-imidazolium salts and their fluorinated derivatives. These salts were characterized using FTIR, 1D and 2D NMR spectroscopy, as well as CHN elemental analysis. Phase transitional properties and phase textures of these amphiphilic salts were studied using DSC and POM.

The cytotoxic effects of these salts against human normal skin fibroblasts (Hs27), cervical cancer cells (HeLa) and/or neuroblastoma (SHSY-5Y), estrogen-positive breast cancer cells (MCF-7), triple negative breast cancer cells (MDA-MB-231) were investigated using the MTT assay. Antimicrobial potentials of these salts against pathogenic Gram-positive bacterium *Staphylococcus aureus* (*S.aureus*), Gram-negative bacteria *Escherichia coli (E.*

coli) and *Salmonella enterica serovar Typhimurium* (*Salmonella*), and yeasts *Candida albicans (C. albicans)* and *Saccharomyces cerevisiae* (*Saccharomyces*) were evaluated using the disc diffusion method.

CHAPTER 2
LITERATURE REVIEW

2.1 An overview of liquid crystals (LCs) and ionic liquid crystals (ILCs)

Liquid crystals (LCs) are a thermodynamically stable state of matter with anisotropy characteristics. LC phases exist in the temperature range between the solid and the isotropic liquid phase, hence they are termed mesophases (Bisoyi & Kumar, 2010; Mani et al., 2022). LC materials are one-of-a-kind in terms of characteristics and applications. LCs play an increasingly essential role in modern technology as research in this field develops and new applications are explored (Douglas, 2016).

LCs were first discovered by F. Reinitzer in 1888 while working with cholesterol derivatives. While elucidating the structures of these esters, unique phase properties of cholesteryl acetate (1) and cholesteryl benzoate (2) (Figure 2.1) were discovered. They had two phase transition temperatures, and each of these compounds had crystal-like optical characteristics but flowed like liquids. Cholesteryl benzoate turned cloudy at 145.5 ℃ and became a clear liquid at 178.5 ℃ (DiLisi, 2019). These phase transitions were completely reversible, and the liquid changed colours upon cooling (Mitov, 2014). Reinitzer confided this discovery to a German physicist, Otto Lehman. A conclusion was reached that a new intermediate state of matter termed ′liquid crystal (LC)′ was discovered.

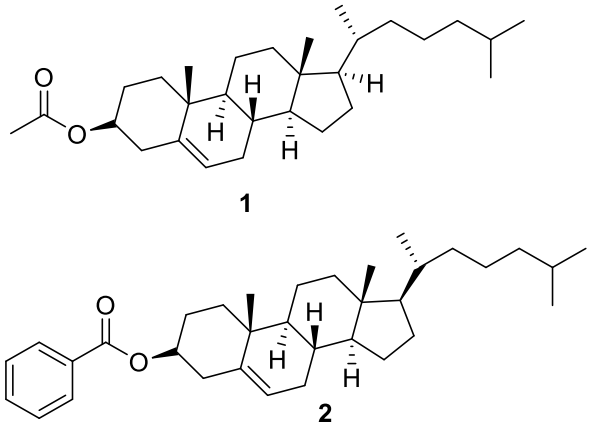

Figure 2.1 Cholesteryl acetate (**1**) and Cholesteryl benzoate (**2**) the first reported liquid crystals (Furrer, 2021; Pérez-Hernández et al., 2018).

Introduction of ionic moieties into neutral LC molecules could lead to the fabrication of ionic liquid crystals (ILCs). ILCs were first reported by Knight and Shaw in 1938, when they discovered the mesomorphic behaviour of some *N*-(n-alkyl)-pyridinium halides (Figure 2.2) (Knight & Shaw, 1938). However, large-scale investigations on ILCs had just begun in the last two decades (Salikolimi et al., 2020). Made up of non-covalently bound cations and anions, ILCs are an intriguing class of LC materials. They have combined anisotropic properties of conventional, neutral LCs (anisotropy, fluidity, self-assembly) and the mobility and self-organization of ILs (ionic, dynamic physical and chemical properties).

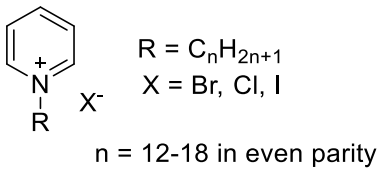

Figure 2.2 *N*-(n-alkyl)-pyridinium halides, the first reported ILCs (Knight & Shaw, 1938).

Cations and anions that are commonly found in ILs are incorporated into the preparation of ILCs. ILCs with aromatic cationic head groups are common and interesting to investigate. The positive charge on aromatic cations could be distributed over a large volume, thus reducing ionic interactions (Goossens et al., 2016). ILCs

based on various aromatic cationic head groups such as imidazolium, pyridinium, and benzimidazolium amongst others, have been reported (Alvarez & Kouwer, 2016; Axenov & Laschat, 2010; Butschies et al., 2013; Goossens et al., 2016) (Figure 2.3). Among the many hitherto reported ILCs, those based on imidazolium and pyridinium salts are the most frequently investigated (Bara et al., 2010; Cao et al., 2020; Kuznetsova et al., 2020; Tang et al., 2019; Wang et al., 2019).

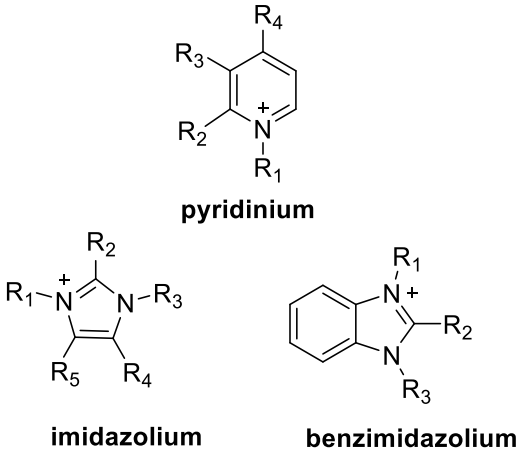

Figure 2.3 Chemical structure of some aromatic cationic head groups

2.1.1 Classification of ILCs: Lyotropic and Thermotropic

Most of the ILCs that have been discovered are rod-shaped or calamitic (Kapernaum et al., 2018). Disc-shaped and banana-shaped mesogens are two other types of ILCs (Goossens et al., 2016; Lutfor et al., 2009). Molecular anisotropy, microsegregation of incompatible units, the aggregation of compatible units and other intermolecular interactions such as ionic and dipole-dipole interactions, H-bonding, π stacking, and van der Waals forces are the driving forces in self-assembly of ILCs (Yu et al., 2009, Alvarez & Kouwer, 2016).

ILCs can be classified into lyotropic and thermotropic (LILCs) and (TILCs). LILCs are amphiphiles comprising of polar hydrophilic cationic head group, attached to nonpolar hydrophobic and/or lipophilic moiety. This class of ILCs exhibits liquid

crystalline properties in certain concentration range. Their LC behaviour is usually controlled by the size of the head groups, number of the alkyl chains in the structures, and the solvent polarity (Goodby, 2004; Huang & Gui, 2018). Thermotropic ILCs (TILCs), on the other hand, are usually rod-like, disc-like or bent (Wang et al., 2020). They are made up of a central polar group connecting two aromatic moieties, and flexible terminal alkyl chains (Nalone et al., 2020). Formation of mesophase(s) in this class of ILCs happens in response to temperature change (Giles et al., 2020; Razali & Jamain, 2021).

2.1.2 Classification of mesophase: smectic, columnar, cubic phases

LC phases can be monotropic or enantiotropic. An enantiotropic LC phase is observed during heating and cooling cycles but monotropic mesophases are observed during the cooling cycle, only due to a hysteresis in crystallization (Rodrigues et al., 2019). LC phases are classified based on the degrees of orientational and positional orders of molecules in the phase. Molecules in LCs phases are preferentially aligned along a particular direction in space. This is referred to as the director and labelled by a unit vector and positional order is the degree to which the position of an average molecule or groups of molecules exhibit translational symmetry (Singh, 2000).

The variety of mesophase formed by ILCs can be distinguished according to those formed by either rod-like or disc-like molecules. This could be smectic, columnar, hexagonal, cubic, or nematic etc (Goossens et al., 2016; Li et al., 2009; PanĂ et al., 2016).

The smectic phase is characterized by an organized layered alignment in rod-like molecules, indicating a connection between its orientation along with positional order. A change in molecular order produces different smectic phases, such as smectic A (SmA), smectic B (SmB), and smectic C (SmC) inclusively (Guillon, 1998).

Formation of a lamellar phase (smectic phase) in ILCs is due to molecular geometry, shape and conformational effects, microsegregation of incompatible units, aggregation of compatible units and volume minimization in mesogen bulk at suitable temperatures. SmA phase is the simplest phase in ILCs. Molecules in this phase are aligned perpendicularly to the plane and arranged in flexible layers (Binnemans, 2005). Another less common phase observed in rod-like ILCs is the SmC phase. This phase is the tilted version of the SmA phase wherein molecules within layers are uniformly tilted with respect to the layer normal.

The columnar phase is a common way of arrangement of discotic molecules. The molecules in the columnar phases are piled one on top of the other to form columns. Columns can be organized in a variety of two-dimensional lattices. The hexagonal columnar phase (Col_h), columnar nematic phase (N_{col}), rectangular columnar phase (Col_r), and the oblique columnar are other forms of columnar phases (Col_o) (Goossens et al., 2016).

Cubic phases are mesophases of cubic symmetry. Their physical properties are no longer anisotropic due to high symmetry. A Long-range positional order (translational symmetry) in three dimensions, which is accompanied with rotational disorder and conformational mobility is usually observed in these phases (Binnemans, 2005; Goossens et al., 2016).

2.2 Effects of fluorination on LC properties

Fluorinated LCs have been actively studied since the 1960s (Bremer et al., 2013). Fluorination has been used as an approach to modify and tune LC properties (Hird & Toyne, 1998). Fluorination was reported to alter the phase transition temperatures, thermal stability, solubility and shape of LCs which in turn regulate their chemical properties, thus allowing the tuning of the physicochemical properties of

LCs. The presence of fluorine atoms also affects other physical properties of LCs such as optical anisotropy, viscoelastic properties, and dielectric anisotropy of LCs. Fluorinated LCs have found applications in a variety of materials, including lubricants and liquid crystal displays (Hird, 2007).

Fluorination can take place at various positions in the LC molecules, for instance the terminal chains and/or lateral positions in the mesogenic cores (Hird & Toyne, 1998). Lateral fluorinated liquid crystalline materials are the most extensively studied (Hird, 2007), and fluorination in the rigid mesogenic cores increases the length to breath ratio of the LC molecules. According to Gray, when molecular width increases, intermolecular cohesiveness may diminish as molecular separation increases (Gray, 1964). Gray was the first researcher to produce laterally fluorinated alkoxyl benzoic acids (**3&4**) (Figure 2.4). The dimers of these acids showed SmC and N phases of reduced stability. The N-Iso phase transition temperature ($T_{N\text{-}Iso}$) was reduced by about 25°C, while the stability of the smectic phase was reduced by 40 °C.

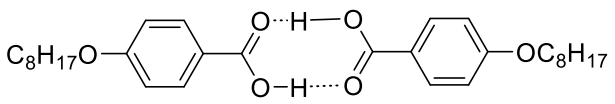

3

Cr 101.0 SmC 108.0 N 147.0 Iso (°C)

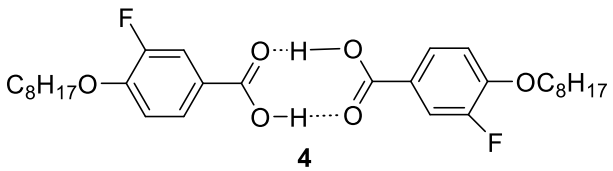

4

Cr 117.0 N 120.5 Iso (°C)

Figure 2.4 Lateral fluorinated alkoxyl benzoic acid (Gray, 1964).

A few decades later, fluorine-substituted benzoate esters linked to an azobenzene core with a terminal double bond (**5-8**) (Figure 2.5) were reported by Rahman and co-workers (Rahman et al., 2014). The phase transition temperatures of

these compounds were found to be about 30°C lower than those of the non-fluorinated analogues.

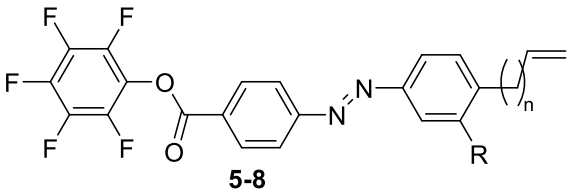

5, n = 1, R = H, Cr 120.5 SmA 114.2 N 169.2 Iso (℃)
6, n = 2, R = H, Cr 129.7 N 161.6 Iso (℃)
7, n = 1, R = F, Cr 99.1 SmA 148.5 Iso (℃)
8, n = 1, R = F, Cr 102.7 SmA 141.9 Iso (℃)

Figure 2.5 Fluorine-substituted benzoate esters linked to an azobenzene core with a terminal double bond (Rahman et al., 2014).

Similar observations were also reported for lateral fluoro-substituted terphenyls with low transition temperatures. Hence lateral fluorination improved the stability of the tilted smectic phase (**9**) (Figure 2.6) (Haouas et al., 2021).

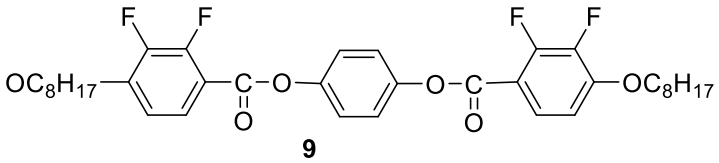

Cr 56.4 SmB 101.5 Iso (℃)

Figure 2.6 Lateral fluoro-substituted terphenyls (Haouas et al., 2021).

2.3 Azobenzene based LCs and ILCs

Azobenzene, an aryl azo compound **10** (Figure.2.7) has the characteristics of aromatic rings and the azo group -N=N-. It is very stable due to the presence of delocalized pi-electrons. The first azobenzene compound was discovered by Eilhard Mitscherlich in 1861, and several years later, in 1937, Hartely reported the impact of light on the -N=N- bond conformation (Hartley, 1937; Merino & Ribagorda, 2012).

Since its discovery, comprehensive research has been carried out to investigate the physical and chemical properties associated with this class of compounds.

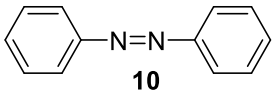

10

Figure 2.7 Chemical structure of azobenzene (Merino, 2011)

Azobenzene derivatives were among the first liquid crystalline compounds identified, with those bearing various substituents being the most investigated (Podruczna et al., 2014). Azobenzene compounds are good LC candidates (Sanches2019). The -N=N- linkage provides flexibility to the two rigid benzene rings. It was discovered that this structural architecture has an impact on their LC characteristics (Yang et al., 2018). Azobenzene based LCs usually exhibit stable mesophases.

Regulation of LC behaviour with light is one of the most intriguing advances in LC science and technology. Light induced modification of molecular conformation is probably the most straightforward way to control LC properties. Anisotropic and photochromic properties have been reported for azobenzene derivatives. Using visible light, these chromophores can be switched between two geometric isomers. Photoisomerization of azobenzene derivatives is fast, reversible, and has a high quantum yield, and the wavelengths at which the transformation occurs can be modified synthetically by adding substituents to the chromophores. Upon isomerization, there can be significant changes to the optical, geometric, mechanical, and chemical properties of the azobenzene molecules (El Halabieh et al., 2004). Their ability to undergo photoisomerization and photochromism was reported to significantly affect the variation in mesophase behaviour (Srinivasa, 2017).

Mesophases can be easily induced in LC materials containing azobenzene chromophores. Their extended aromatic π-systems enhance mesomorphism (Madiahlagan et al., 2019). The *trans* form of azobenzene derivatives has a rod-like shape that can stabilise a LC phase, whereas the cis form has a bent-like conformation that destabilises the LC superstructure by causing disorder in aligned systems (He et al., 2018). Since these materials are facile to synthesise and their shape anisotropy is favourable for the development of LC phases, the photoactive bistable azobenzene moiety is commonly inserted in calamitic (rod-shape) or banana-shape mesogens (Ahmed et al., 2016).

Azobenzene ILCs are prepared via incorporation of ionic moieties into neutral azobenzene LCs impart amphiphilicity onto and improve solubility of these salts in organic solvents. These ionic moieties also promote the formation of smectic phases. They exhibit lower melting temperatures and unique mesophase when compared to neutral azobenzene LCs. For example, the presence of a cationic ammonium head group in the first azobenzene ILCs (Figure 2.8) was reported to promote and enhance the stability of the SmA phase in the work of Ujiie and Iimura (Ujiie & Iimura, 1992). This team compared neutral LC derivative of azobenzene (**11**) with ionic counterpart. Neighbouring mesogenic groups in (**12-14**), when compared to their neutral counterpart (**11**), was described to overlap each other and the cationic ammonium heads aggregated to produce a sublayer in the smectic layer, thus the stability was enhanced. Generally, there was a decrease in the melting temperatures in **12-14**, and an increase in mesophase-isotropization temperatures when compared to **11**.

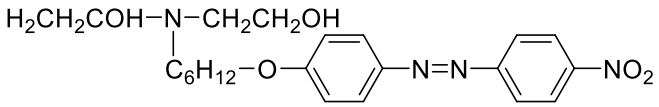

11

Cr 61.2 SmA 119.8 Iso (°C)

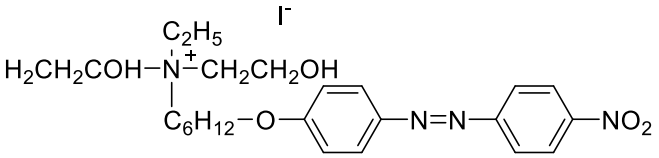

12

Cr 40.5 SmA 170.2 Iso (°C)

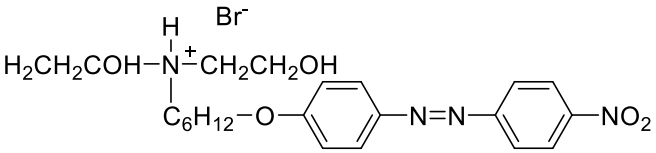

13

Cr 56.9 SmA 207.0 Iso (°C)

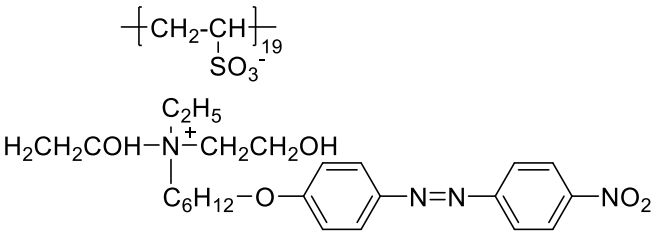

14

Cr 50.0 SmA 235.0 Iso (°C)

Figure 2.8 Chemical structure of ammonium-containing azobenzene ILCs with enhanced phase stability (Ujiie & Iimura, 1992)

In 1994, Ujiie & Iimura synthesized another neutral and azobenzene ILCs containing cationic ammonium head group and a chiral hydrogen tartrate as the anion (**15&16**) (Figure 2.9). A homeotropic SmA phase was recorded for the neutral compound (**15**) upon cooling from the isotropic phase, and SmC phase upon further cooling due to the formation of the tilted layered structure. Transition temperatures recorded were higher in the ionic salt (**16**) than the neutral counterpart thus leading to a higher mesophase stability, and a chiral SmC* phase was documented in addition to SmA phase in the compound. The difference in the SmA-isotropic transition

temperatures of the compounds was attributed to the formation of ionic aggregates by the cationic ammonium headgroup contained in **16** (Ujiie & Iimura, 1994).

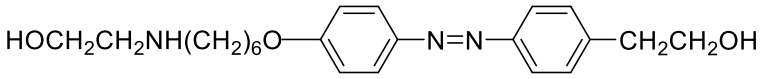

15

Cr 74.6 SmC 94.7 SmA 144.7 Iso (°C)

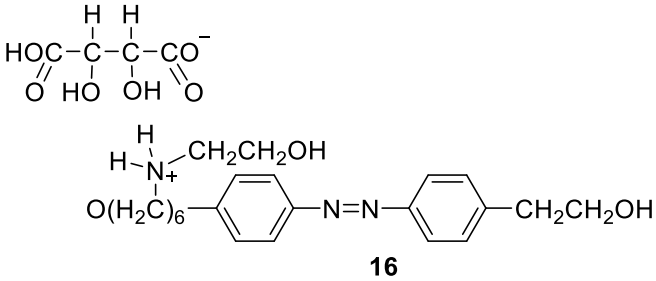

16

Cr 50.5 SmC* 105.0 SmA 175.0 Iso (°C)

Figure 2.9 Neutral and azobenzene ILCs containing cationic ammonium head group and a chiral hydrogentartrate as the anion (Ujiie & Iimura, 1994)

A few years later, the same group reported some neutral, and cationic *N*-2-hydroxyethylpiperidinium containing azobenzene ILCs (**17-19**) as shown in Figure 2.10. The neutral compounds were reported to exhibit monotropic SmA phase while the ionic counterparts were documented to form enantiotropic SmA phase. These salts showed higher clearing points when compared to the neutral compounds. Ionic aggregation was reported to be an important factor in the LC behaviour of the compounds (Ujiie et al., 2006).

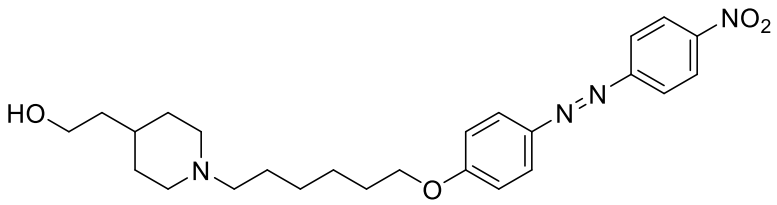

17

Cr 72.8 SmA 103.0 Iso (°C)

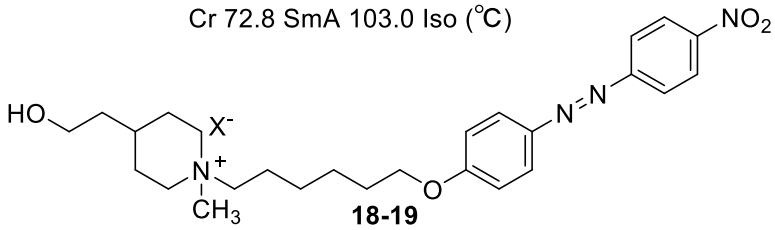

18-19

18, X = I^-, SmAg 32.9 SmA 149.3 Iso (°C)

19, X = Br^-, Cr 78.3 Sm 172.1 Iso (°C)

Figure 2.10 Neutral and cationic N-2-hydroxyethylpiperidinium containing azobenzene ILCs (Ujiie et al., 2006)

Molecular interactions could be adjusted to obtain the desired liquid crystalline behaviour in azobenzene ILCs. This was demonstrated by Li and co-workers, where the influence of a branched molecular geometry and terminal alkyl chain length was studied for phase transition and mesophase type in some calamitic azobenzene derivatives (Li et al., 2009). The mesogenic unit was laterally linked to an ammonium group in forming a T-shaped ILC (**20-23**) (Figure 2.11). The rare N phase in ILCs, and SmA phase were documented for the compounds. The maximum chain length of compounds that exhibited the N phase was eight carbons atoms. The phase transition temperature of these compounds from G (glass transition) to mesophase and subsequent isotropy was reported to rise accordingly with an increase in the alkyl chain length.

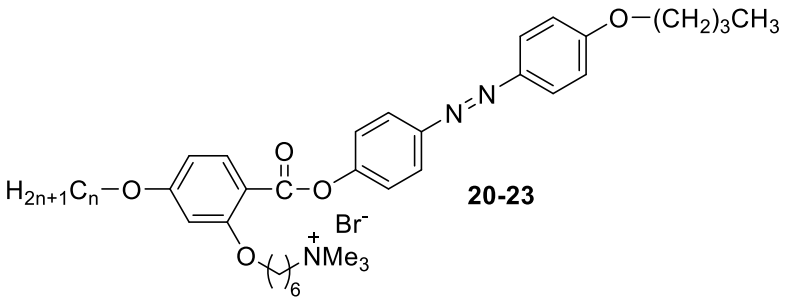

20, n = 6 G 23 N 36 Iso (°C)
21, n = 8 G 25 N 68 Iso (°C)
22, n = 10 G 32 SmA 87 Iso (°C)
23, n = 12 G 32 SmA 92 Iso (°C)

Figure 2.11 T-shaped azobenzene ILCs prepared by Li and co-workers (Li et al., 2009).

The linking group e.g alkyl spacer between the cationic head and the mesogenic core could also influence the LC behaviour of ILCs. For instance, Wuckert and co-workers synthesized some azobenzene ILCs containing a cationic guanidinium head group with an alkyl spacer length of 3-8 carbon atoms to the azo-core (**24-29**) (Figure 2.12). The compounds were reported to exhibit the enantiotropic SmA phase irrespective of alkyl spacer length. However, melting and clearing temperatures were reportedly observed to increase from a spacer length of 3-5 carbon atoms, decreased from 6 to 8 carbon atoms and the mesophase stability remained similar in the compounds (Wuckert et al., 2015).

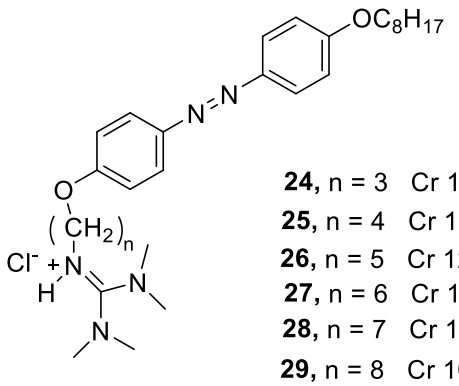

24, n = 3 Cr 118 SmA 139 Iso (°C)
25, n = 4 Cr 125 SmA 151 Iso (°C)
26, n = 5 Cr 125 SmA 150 Iso (°C)
27, n = 6 Cr 117 SmA 137 Iso (°C)
28, n = 7 Cr 111 SmA 129 Iso (°C)
29, n = 8 Cr 100 SmA 125 Iso (°C)

Figure 2.12 Chemical structures of azobenzene-guanidinium ILCs (Wuckert et al., 2015)